This is a "preproof" accepted article for *Mineralogical Magazine*.
This version may be subject to change during the production process.
10.1180/mgm.2025.14

Cummingtonite-($P2_1/m$): Crystal-structure refinement, Mössbauer spectroscopy and infrared spectroscopy, and some aspects of classification of the magnesium-iron-manganese amphiboles

Frank C. Hawthorne[1,*], Andrew R. Lapierre[1], Yassir Abdu[1,3], Roberta Oberti[2] and Maxwell C. Day[1,4]

[1] Department of Earth Sciences, University of Manitoba, Winnipeg, Manitoba R3T 2N2, Canada
[2] CNR-Istituto di Geoscienze e Georisorse, unità di Pavia, via Ferrata 1, I-27100 Pavia, Italy
[3] Current address: Department of Applied Physics and Astronomy, University of Sharjah, P.O. Box 27272, Sharjah, United Arab Emirates
[4] Current address: Department of Geosciences, University of Padova, 35131 Padova, Italy

Running title: Cummingtonite-($P2_1/m$): Crystal-structure and spectroscopy

* Corresponding author, E-mail address: frank.hawthorne@umanitoba.ca

Abstract

The crystal structure of cummingtonite-($P2_1/m$) was characterized by single-crystal structure-refinement, infrared spectroscopy and ^{57}Fe Mössbauer spectroscopy. Previous cummingtonite-($P2_1/m$) specimens characterized have Mn^{2+} as the dominant constituent at $M(4)$ but this amphibole has Fe^{2+} dominant at $M(4)$. The formula of the amphibole was corrected for minor exsolved calcium-amphibole and is $(Mg_{5.66}Fe^{2+}_{1.28}Mn_{0.06})_{\Sigma=7.00}Si_{8.00}O_{22}(OH)_2$. The crystal structure, a = 9.4885(19), b = 18.040(4), c = 5.2891(11) Å, β = 102.06(3)°, V = 885.4(3) Å^3, space group $P2_1/m$, Z = 2, was refined to an R_1-index of 3.34% for 2338 observed reflections. Site-occupancy refinement gave the following site-populations: $M(1)$ = 1.972(8) Mg + 0.028 Fe^{2+}, $M(2)$ = 2.000 Mg, $M(3)$ = 0.989(6) Mg + 0.011 Fe^{2+}, $M(4)$ = 0.815(8) Mg + 1.125 Fe^{2+} + 0.060 Mn^{2+} apfu. Infrared spectroscopy in the principal (OH)-stretching region shows two peaks at 3367 and 3652 cm^{-1} that were assigned to the local arrangements $^{M(1)}Mg^{M(1)}Mg^{M(3)}Mg$–OH

and $^{M(1)}Mg^{M(1)}Fe^{2+}{}^{M(3)}Mg$–OH (≈ $^{M(1)}Mg^{M(1)}Mg^{M(3)}Fe^{2+}$–OH) with relative intensities in accord with the refined site-populations. ^{57}Fe Mössbauer spectrum shows three quadrupole-split doublets with parameters indicative of octahedrally coordinated Fe^{2+} at *M*(4) and *M*(1,2,3), and octahedrally coordinated Fe^{3+} that occurs in exsolved calcium amphibole. All three techniques indicate a small amount of Fe^{2+} at *M*(1,2,3) despite the fact that there is more than sufficient ^{C}Mg to completely fill the *M*(1,2,3) sites: 5.66 Mg pfu. Issues involving the current and possible future nomenclature and classification of the magnesium-iron-manganese amphiboles are discussed in detail.

Keywords: Amphibole, cummingtonite-($P2_1/m$), single-crystal structure-refinement, infrared spectroscopy, ^{57}Fe Mössbauer spectroscopy, Mg^{2+}–Fe^{2+} order-disorder.

Introduction

The general chemical formula of the amphiboles may be written (Hawthorne and Oberti, 2007a,b) as

$$A\ B_2\ C_5\ T_8\ O_{22}\ W_2$$

where A = □, Na^+, K^+, Ca^{2+}, Pb^{2+}, Li^+;
B = Na^+, Ca^{2+}, Mn^{2+}, Fe^{2+}, Mg^{2+}, Li^+;
C = Mg^{2+}, Fe^{2+}, Mn^{2+}, Al^{3+}, Fe^{3+}, Mn^{3+}, Cr^{3+}, Ti^{4+}, Li^+;
T = Si^{4+}, Al^{3+}, Ti^{4+}, Be^{2+};
W = (OH), F, Cl, O^{2-}.

Atoms and ions are indicated by Roman symbols (*e.g.* Si^{4+}, Si), groups of atoms or ions are indicated by upper-case Roman letters (as in the general formula above); crystallographic sites are indicated by italicized symbols, *e.g.* *T*(1), *M*(4); polyhedra are labelled by the central site, *e.g.* *T*(1) tetrahedron, *M*(4) polyhedron. Data are presented here for cummingtonite-$P2_1/m$, the structure of which is illustrated in Fig. 1. Where discussing the refinement of site occupancies, atoms are written as neutral because neutral scattering factors were used in the crystal-structure refinement.

The IMA-CNMNC rules for naming and classifying amphiboles (Hawthorne *et al.*, 2012, henceforth referred to as IMA2012) are currently under revision. One of the proposed changes involves the criteria for naming and classifying the magnesium-iron-manganese amphiboles which are currently considered as a single amphibole subgroup. It was well-known at the time that both Mn^{2+} and Fe^{2+} are strongly ordered at the *M*4 and *M*(4) sites in orthorhombic and monoclinic amphiboles, respectively, but ^{B}Mg, $^{B}Fe^{2+}$ and $^{B}Mn^{2+}$ were not introduced as

classification parameters because of the considerable increase in complexity of the classification and the negative impact that the Amphibole Subcommittee felt that this would have on the petrology community. Any changes to the IMA2012 nomenclature and classification of the magnesium-iron-manganese amphiboles will have several very significant effects and the intent of the current paper is to consider these possible effects prior to any change in nomenclature and classification. The cummingtonite-$P2_1/m$ described by Kisch (1969) is ideal for this purpose and a more detailed crystallographic and spectroscopic characterization is given here.

The $P2_1/m$ amphibole structure

The $P2_1/m$ structure is shown in Fig. 1. There are four distinct *T*-sites, *T*(1A), *T*(1B), *T*(2A) and *T*(2B), that are tetrahedrally coordinated and link to form two distinct types of double-chain of tetrahedra, the A-chain and the B-chain. Coordination and linkage of these *T* sites is analogous to that in the *C*2/*m* amphibole structure. The A- and B-chains face each other back-to-back across the A cavity, and the B-chain is much more kinked than the A-chain (Fig. 1). There are three distinct *M* sites that are occupied by the C cations, *M*(1), *M*(2) and *M*(3) with point symmetries 1, 1 and *m*, respectively. The *M*(4) site has point symmetry 1 and eight adjacent oxygen atoms. However, the cations occupying this site may not bond to all surrounding oxygen atoms, and the existence of this structure type seems to depend on the bonding requirements of the *M*(4) cation and the surrounding oxygen atoms.

Some synthetic amphiboles have $P2_1/m$ symmetry and one synthetic amphibole with $C\bar{1}$ symmetry (Cámara et al., 2004) have been reported. The nature of the $P2_1/m$–$C2/m$ transition has been studied in considerable detail: $Na(NaMg)Mg_5Si_8O_{22}(OH)_2$ (Cámara *et al.,* 2003; Iezzi *et al.,* 2004); $Na(NaMg)Mg_5Si_8O_{22}F_2$ (Cámara *et al.,* 2008); $^{A}Na^{B}(LiMg)^{C}Mg_5Si_8O_{22}(OH)_2$ (Iezzi *et al.,* 2005a); $Na(NaMg)Mg_5Si_8O_{22}(OH)_2$ – $Na(LiMg)Mg_5Si_8O_{22}(OH)_2$ solid-solutions (Iezzi *et al.,* 2006); and $Na(NaMg)Mg_5Si_8O_{22}(OH)_2$ – $Na(NaCa)Mg_5Si_8O_{22}(OH)_2$ solid-solutions (Iezzi *et al.,* 2010, 2011). Welch *et al.* (2007) has reviewed the atomic-scale mechanisms of these transitions in detail.

Previous work: general

The magnesium-iron-manganese amphiboles are an important subgroup within the hierarchical classification of the amphiboles (Hawthorne, 1983; Hawthorne *et al*., 2012) and have the general formula $^{A}(\square,Na)\ ^{B}(Mg, Fe^{2+},Mn^{2+})\ ^{C}(Mg,Fe^{2+},Mn^{2+},Al,Fe^{3+})\ ^{T}(Si,Al)_8\ O_{22}\ ^{W}(OH)_2$. They may be orthorhombic and monoclinic with space groups *Pnma*, *Pnmn*, *C*2/*m* and $P2_1/m$

(Hawthorne and Oberti, 2007a) and the more common compositions range from anthophyllite to gedrite (Rabbitt, 1948; Robinson and Jaffe, 1969; Robinson *et al*., 1971; Hawthorne *et al*., 2008; Schindler *et al*., 2008) and from cummingtonite to grunerite (Winchell, 1938; Mueller, 1960; Klein, 1964). Extensive crystallographic (Papike and Ross, 1970; Hawthorne *et al.*, 2008; Schindler *et al*., 2008; Viswanathan and Ghose, 1965; Klein and Waldbaum, 1967; Hafner and Ghose, 1971), optical (Evans and Medenbach, 1997) and thermodynamic (Evans and Ghiorso, 1995; Ghiorso *et al*., 1995) work has been done on both orthorhombic and monoclinic structures.

Previous work: *P*2$_1$/*m* magnesium-iron-manganese amphiboles

Bown (1966) first identified cummingtonite with *P*2$_1$/*m* symmetry occurring as fine exsolution lamellae in tremolite from the Wight Talc Mine, Adirondacks, New York State, USA. Papike *et al.* (1969) refined the structure of a cummingtonite with *P*2$_1$/*m* symmetry and stated that "The *M*(1), *M*(2) and *M*(3) sites are virtually filled by Mg in the primitive structure, according to our refinement", in agreement with an unpublished infrared spectrum, although they give no detailed results of a site-occupancy refinement. Prewitt *et al.* (1970) report the structure of the same sample with all Mn^{2+} and Fe^{2+} assigned to the *M*(4) site: *M*(1,2,3) = $Mg_{5.00}$, *M*(4) = $Mn^{2+}_{0.98}Ca_{0.30}Fe_{0.02}Mg_{0.56}Na_{0.06}$ apfu (atoms per formula unit). Ghose and Yang (1989) refined the structure of a *C*2/*m* amphibole with the formula $(Ca_{0.24}Mn_{2.41}Mg_{4.20}Fe_{0.15})Si_8O_{22}(OH)_2$ from Nsuta, Ghana; the *M*(4) site is dominated by Mn (although the small amount of Fe was not considered in the assignment of site populations) and small amounts of Mn occur at the *M*(1,2,3) sites as forced by the chemical formula. Thus at some composition intermediate between $^{M(4)}$Mn = 0.89 apfu (Prewitt *et al.*, 1970) and $^{M(4)}$Mn = 1.67 apfu (Ghose and Yang, 1989), the structure must change from *P*2$_1$/*m* to *C*2/*m* symmetry at room temperature.

Roy (1981) noted that Mn-rich cummingtonite is a common constituent of Mn ore-deposits with compositions containing less than ~2.3 Mn^{2+} apfu. Maresch and Czank (1983) synthesized orthorhombic amphiboles of composition $Mn^{2+}_xMg_{7-x}[Si_8O_{22}](OH)_2$ with $0.2 < Mn^{2+} < 2.3$ apfu and noted that, unlike their natural monoclinic compositional analogues, these synthetic amphiboles contain abundant chain-width and chain-arrangement faults. Conversely, Dasgupta *et al*. (1985) determined the stability of monoclinic amphibole (space group not determined) of composition $Mn^{2+}_{2.35}Mg_{4.65}[Si_8O_{22}](OH)_2$ at ~100–170°C lower than did Maresch and Czank (1983), and this temperature difference may account for the difference in the character of the synthesized amphiboles.

Previous work: The *P*2$_1$/*m*–*C*2/*m* transition in magnesium-iron-manganese amphiboles

Much work has been done on crystallographic aspects of the *P*2$_1$/*m*–*C*2/*m* transition in magnesium-iron-manganese amphiboles. This work focused on the structural changes associated with the transition between the two different structure types as a function of temperature (Prewitt *et al*., 1970; Sueno *et al*., 1972; Yang and Hirschmann, 1995; Yang and Smyth, 1996), chemical composition (Reece *et al.,* 2000, 2002) and pressure (Yang *et al*., 1998; Boffa Ballaran *et al*., 2000). Later work has focused on the thermodynamic aspects of the *P*2$_1$/*m*–*C*2/*m* transition (Boffa Ballaran *et al*., 2000, 2001, 2002, 2004; Reece *et al.,* 2000, 2002) via the behaviour of the order parameter through the phase transition. Note that the property of *P*2$_1$/*m* symmetry does not warrant an amphibole being considered as a distinct species; species definitions depend on chemical composition although the suffix "-*P*2$_1$/*m*" is appended to the name of the amphibole or synthetic amphibole where appropriate. Thus monoclinic magnesium-iron-manganese amphiboles with Mn^{2+} and Fe^{2+} dominant at the *M*(4) site are recognized by IMA2012 as distinct species but have no names as, although they are relatively common in Nature, they have not been formally described, proposed and approved by IMA-CNMNC as new mineral species. *Monoclinic magnesium-iron-manganese amphiboles with Mg dominant at M(4) are not recognized as distinct species because no natural (unheated) examples have yet been discovered and laboratory-heated minerals are no longer considered as minerals by IMA-CNMNC* (with the exception of heated metamict minerals). All amphibole minerals with *P*2$_1$/*m* symmetry at room temperature refined thus far have Mn^{2+} or Fe^{2+} as the dominant cation at the *M*(4) site. Some chemical compositions have been reported that purportedly have very low Fe / (Fe + Mg) ratios but closer inspection shows this not to be the case: *e.g*. (1) the amphibole occurs as lamellae in tremolite too small to analyze by electron microprobe and the Fe / (Fe + Mg) ratio reported is that of tremolite; (2) the amphibole is orthorhombic, not monoclinic.

Kisch (1969) reported cummingtonite of composition $Na_{0.09}(Ca_{0.19}Mg_{5.45}Fe^{2+}_{1.23}Mn^{2+}_{0.04}Ti^{4+}_{0.01}Al_{0.07})(Si_{7.83}Al_{0.17})O_{22}(OH)_2$ with *P*2$_1$/*m* symmetry at room temperature. As this is the room-temperature cummingtonite with the most Mg at *M*(4) (see compilation of analyses in Table 1 of Welch *et al.,* 2007), we deemed it worthy of further examination.

Sample provenance

A colourless magnesium-iron-manganese amphibole is associated with a pale bluish-green calcium amphibole and chlorite in a small irregular mass of metamorphosed ultramafic rock within the "granitized zones" west of the Cooma granite-gneiss, Cooma, New South Wales (Joplin, 1942). Kisch (1969) identified the colourless amphibole as cummingtonite-(*P*2$_1$/*m*).

Chemical composition

We have used the chemical analysis of cummingtonite-($P2_1/m$) (Table 1) determined by electron-microprobe analysis by Kisch (1969). The empirical chemical formula (Table 1) was calculated on the basis of 24 (O + OH + F) with OH + F = 2 apfu and Fe^{3+} = 0.10 apfu as indicated by Mössbauer spectroscopy.

Infrared spectroscopy

For single-crystal FTIR spectroscopy, a transmission spectrum was collected using a Bruker Hyperion 2000 IR microscope equipped with a liquid-nitrogen-cooled MCT detector. The sample was prepared as a thin film using a diamond micro-compression cell. Data over the range (4000–650 cm^{-1}) were obtained by averaging 100 scans with a resolution of 4 cm^{-1}. Base-line correction and spectral fitting (with a Gaussian function) were done using the program Fityk (Wojdyr, 2010). Fig. 2 shows the infrared spectrum of cummingtonite-($P2_1/m$) in the principal OH-stretching region fit to two bands with half-widths of 10 cm^{-1} and fitting parameters as listed in Table 2.

Mössbauer spectroscopy

The Mössbauer spectrum was acquired in transmission geometry at room temperature using a ^{57}Co(Rh) point source, and the spectrometer was calibrated with the room-temperature spectrum of α–Fe. The spectrum was analyzed in terms of a Voigt-function-based quadrupole-splitting distribution (Rancourt and Ping, 1991) using the RECOIL® software package. Fig. 3 shows the Mössbauer spectrum of cummingtonite-($P2_1/m$) fit to three bands and details of the fitted spectrum are given in Table 3.

Crystal-structure refinement

A crystal was attached to a tapered glass fibre and mounted on a Bruker D8 three-circle diffractometer equipped with a rotating-anode generator (Mo$K\alpha$ radiation), multilayer optics and an APEX-II detector. A total of 31960 intensities was collected to 65° 2θ using 6 s per 0.3° frame, with a crystal-to-detector distance of 5 cm. Empirical absorption corrections (SADABS; Sheldrick, 2008) were applied and reflections were corrected for Lorentz, polarization and background effects, averaged and reduced to structure factors. The unit-cell dimensions were refined by least-squares from the positions of 4061 reflections with $I > 10\sigma I$ and are given in Table 4, together with other information on data collection and structure refinement. All

calculations were done with the SHELXTL PC (Plus) system of programs; *R* indices are expressed as percentages. The structure was refined to convergence by full-matrix least-squares methods with anisotropic-displacement parameters for all atoms except the H atoms. At the later stages of refinement, difference-Fourier maps showed weak density maxima approximately 1 Å from the O(3A) and O(3B) anions. These maxima were entered into the refinement as H atoms and their positional parameters were refined with the restraint that the O(3A)–HA and O(3B)–HB distances be approximately 0.96 Å. In crystal structures refined by X-ray diffraction, the O_{donor}–H distances obtained are too short as a significant fraction of the electron density of H is delocalised into the O_{donor}–H bond. This has the effect of giving poor H…$O_{acceptor}$ hydrogen-bond distances, often making it difficult to interpret the role of hydrogen bonds in a structure. This may be avoided by restraining the O_{donor}–H distances during refinement to their expected values based on neutron diffraction. In the present case, the O_{donor}…H distances were restrained to 0.96 Å, close to the O_{donor}–H distances found by neutron diffraction for tremolite (Hawthorne and Grundy, 1976) and kaersutite (Gatta *et al*., 2017). The structure converged to a final R_{obs} index of 3.34%. Refined atom coordinates and anisotropic-displacement parameters are listed in Table 5, and selected interatomic distances are given in Table 6. The crystal structure of cummingtonite-($P2_1/m$) is illustrated in Fig. 1 and will be helpful in discussions involving bond lengths and cation order. A table of structure factors and a Crystallographic Information File (CIF) for cummingtonite-($P2_1/m$) have been deposited with the Principal Editor of *Mineralogical Magazine* and are available as Supplementary Material (see below).

Derivation of site populations

The chemical analysis of Table 1 lists significant Na as an A-group cation. However, there was no significant density in the *A*-cavity at the final stages of refinement and attempts to insert ^{A}Na and refine its occupancy led to near-zero occupancy and nonsensical atom coordinates. As stated in the section on sample provenance, cummingtonite-($P2_1/m$) is associated with a pale bluish-green calcium amphibole. Coexisting magnesium-iron-manganese- and calcium-amphiboles generally show mutual exsolution (*e.g.* Asklund *et al*., 1962; Jaffe *et al*., 1968; Ross *et al*., 1969; Klein *et al*., 1996). Let us examine the formula from Table 1 (modified for the amount of Fe^{3+} determined here by Mössbauer spectroscopy, Table 3, Fig. 3): $Na_{0.11}(Ca_{0.14}Mg_{5.57}Fe^{2+}_{1.16}Mn_{0.06}Fe^{3+}_{0.10})_{7.03}(Si_{7.86}Al_{0.11})_{7.97}O_{22}(OH)_2$. The constituents of this formula that do not fit the form $(Mg,Fe^{2+},Mn)_7Si_8O_{22}(OH)_2$ are $^{A}Na_{0.11}{}^{B}Ca_{0.14}{}^{C}Fe^{3+}_{0.10}{}^{T}Al_{0.11}$. These constituents we may reasonably assign to calcium amphibole exsolved from cummingtonite-

($P2_1/m$), particularly as no density was observed at the *A*-site and attempts to refine Na at the *A*-site were unsuccessful. If we remove these extra constituents from the formula and renormalize, we get the following formula for cummingtonite-($P2_1/m$): $(Mg_{5.66}Fe^{2+}_{1.28}Mn_{0.06})_{\Sigma=7.00}Si_{8.00}$.

The refined <*T*–O> distances (Table 6) are in accord with the lack of Al at the *T* sites. As expected, Fe^{2+} is strongly ordered at the *M*(4) site relative to the *M*(1,2,3) sites (Table 7). The Fe^{2+} content at *M*(2) refined to very close to zero and was set at this value in the final stages of refinement. Small positive occupancies for Fe^{2+} at *M*(1) and *M*(3) were obtained with a preference for *M*(1).

Cation order from infrared and Mössbauer spectroscopies

The fitted infrared spectrum in the principal OH-stretching region is shown in Fig. 2 and details regarding the fitted spectrum are given in Table 2. The spectrum has a strong symmetrical peak at 3667 cm^{-1} and a much weaker peak at 3653 cm^{-1}. These peaks are assigned to configuration symbol $^{M(1)}M^{2+}\,^{M(1)}M^{2+}\,^{M(3)}M^{2+}$–OH–$^{A}\square$–$^{T}Si\,^{T}Si$ (Hawthorne and Della Ventura, 2007) which simplifies to $^{M(1)}M^{2+}\,^{M(1)}M^{2+}\,^{M(3)}M^{2+}$–OH as the other sites are completely ordered, and the resulting local arrangements are $^{M(1)}Mg\,^{M(1)}Mg\,^{M(3)}Mg$–OH and $^{M(1)}Mg\,^{M(1)}Fe^{2+}\,^{M(3)}Mg$–OH (≈ $^{M(1)}Mg\,^{M(1)}Mg\,^{M(3)}Fe^{2+}$–OH) in accord with Burns and Strens (1966) and Strens (1974). In the $P2_1/m$-amphibole structure, there are two distinct (OH) groups (Table 5), O(3A) associated with HA and O(3B) associated with HB, and each local arrangement around each distinct (OH) group will give rise to two peaks of (approximately) the same intensity. In some other $P2_1/m$ amphibole structures, this is the case: in both synthetic $^{A}Na^{B}(LiMg)^{C}Mg_5Si_8O_{22}(OH)_2$ and synthetic $Na(NaMg)Mg_5Si_8O_{22}(OH)_2$ (Iezzi *et al.,* 2005a,b), there are two well-resolved peaks assigned to the local arrangement $^{M(1)}Mg\,^{M(1)}Mg\,^{M(3)}Mg$–OH (Table 8). However, in cummingtonite-($P2_1/m$) (this work), there is a single peak at 3667 cm^{-1} with a half-width of 10 cm^{-1}, resembling the spectrum of *C*2/*m* cummingtonite (Reece *et al.,* 2000; Boffa Ballaran *et al.,* 2004) (Table 8). We may get a measure of the strengths of the hydrogen bonds in amphiboles with *M*(1,2,3) ≈ 5 apfu by examining the *M*(1,2,3)–OH distances: the shorter the bonds from ^{C}Mg to the (OH) group, the stronger the O_{donor}–H bonds, the higher the principal-stretching frequency, and the weaker the H…$O_{acceptor}$ hydrogen bond. In synthetic $Na(NaMg)Mg_5Si_8O_{22}(OH)_2$ (Table 8), the <O3A–Mg_3> and <O3B–Mg_3> distances are very different: 1.996 and 2.030 Å, respectively, indicating that the corresponding peaks in the infrared should be well-resolved, as is the case (Table 8). In cummingtonite-($P2_1/m$) and cummingtonite (Table 8), the corresponding <O3A–Mg_3>, <O3B–Mg_3> and <O3–Mg_3> distances are very similar: 2.075, 2.063 and 2.061 cm^{-1} with very close half-widths: 10 and 8 cm^{-1}, respectively. The similarity of these values and their considerable

difference from those of $Na(NaMg)Mg_5Si_8O_{22}(OH)_2$ suggest that there is a small difference in the frequencies of the peaks corresponding to the O3A–HA and O3B–HB arrangements. This peak separation is small compared to the half-widths of the peaks, and results in overlap of the two peaks in the spectrum of cummingtonite-($P2_1/m$) with just a slight broadening of the resultant composite peak.

The Mössbauer spectrum (Fig. 3) shows three quadrupole-split doublets. The dominant doublet and the intermediate-intensity doublet may be assigned to octahedrally coordinated Fe^{2+} at *M*(4) and *M*(1,2,3), respectively, in accord with Bancroft ***et al.*** (1967), Hafner and Ghose (1971), Ghose and Weidner (1972) and Barabanov and Tomilov (1973). The weakest doublet has a much lower centre shift (0.37 mm/s, Table 3), indicative of octahedrally coordinated Fe^{3+} (Hawthorne, 1988) that occurs in exsolved calcium amphibole. Both the infrared spectrum and the Mössbauer spectrum are in accord with the strong order of Fe^{2+} at *M*(4) but also a small amount of Fe^{2+} at *M*(1,2,3) as indicated by the structure refinement.

The argument for a revised classification for the magnesium-iron-manganese amphiboles

Some years ago, there was external pressure on IMA-CNMNC to include ^{B}Mg, $^{B}Fe^{2+}$ and $^{B}Mn^{2+}$ as classification criteria, and the chair of IMA-CNMNC at the time directed the Amphibole Subcommittee to revise IMA2012 in this respect. This revision has raised some tricky issues concerning the classification of amphiboles (and minerals in general) and the senior (oldest) author of both this paper and IMA2012 thought it appropriate to air these issues in the scientific literature prior to possible implementation.

The current classification of the magnesium-iron-manganese amphiboles

Table 9 shows the current IMA2012 classification of the magnesium-iron-manganese amphiboles. When most amphiboles are analyzed, their site occupancies are not determined and cations are assigned to the A-, B-, C- and T-groups in the following order: (1) T: Si, Al, Ti^{4+}; (2) C: Ti^{4+}, Al, Fe^{3+}, Mn^{3+}, V^{3+}, Cr^{3+}, Mg, Fe^{2+}, Mn^{2+}, Li; (3) B: Mn^{2+}, (Fe^{2+}, Mg), Li, Ca, Na; (4) A: Ca, Na, K. From the work cited above, it was recognised over 50 years ago that Mn^{2+} shows a strong preference for the *M*(4) site in monoclinic magnesium-iron-manganese amphiboles. The relative amounts of Mg and Fe^{2+} in the B- and C-cation groups of the magnesium-iron-manganese amphiboles cannot be determined without crystal-structure refinement or Mössbauer or infrared spectroscopy. Hence for this subgroup, IMA2012 treated the divisions between Mg–Fe^{2+} homovalent analogues in terms of the sum of the B and C cations. However,

it was recognized that Mn^{2+} has a significant preference for the *M*(4) site, and hence distinct species were recognized in IMA2012 with Mn^{2+} assigned as the dominant B-cation with the rider that "where direct experimental data are available, they take precedence over such an assignment".

An alternative classification

For amphiboles of the cummingtonite-grunerite series, Hirschmann *et al.* (1994) and Evans *et al.* (2001) showed that Fe^{2+} is very strongly ordered at the *M*(4) site (Fig. 4), relative to the *M*(1,2,3) sites. Orthorhombic magnesium-iron amphiboles (anthophyllite – "ferro-anthophyllite") show analogous behaviour (Seifert, 1978). In Fig. 4, the red diamonds show compositions of unheated amphiboles of the cummingtonite-grunerite series of Hirschmann *et al.* (1994). IMA2012 treats these compositions as having complete disorder of Mg and Fe^{2+} between the B- and C-groups of cations, *i.e*. the *M*(4) and *M*(1,2,3) sites; according to this model, the data should follow the straight broken black line in Fig. 4. There is no correlation between the behaviour of the data (red diamonds) and the model used by IMA2012; the latter is obviously not adequate. An alternative model to that used by IMA2012 is as follows: C-group cations are assigned as indicated above, and if the total amount exceeds 5 apfu, the cations are assigned to the B-group in the following order: Mn^{2+}, Fe^{2+}, Mg^{2+}. When this is done, the site-occupancy data will follow the solid green lines in Fig. 4 which are in much closer accord with the experimental data than the assignment used in IMA2012.

Solid solution in magnesium-iron-manganese amphiboles

It has been customary in the past to regard the compositional range $Mg_7Si_8O_{22}(OH)_2$ – $Fe^{2+}{}_7Si_8O_{22}(OH)_2$ in monoclinic amphiboles as a binary solid-solution series. However, it is better considered as two separate solid-solution series, ${}^{B}Mg_2{}^{C}Mg_5Si_8O_{22}(OH)_2$ – ${}^{B}Fe^{2+}{}_2{}^{C}Mg_5Si_8O_{22}(OH)_2$ and ${}^{B}Fe^{2+}{}_2{}^{C}Mg_5Si_8O_{22}(OH)_2$ – ${}^{B}Fe^{2+}{}_2{}^{C}Fe^{2+}{}_5Si_8O_{22}(OH)_2$ as the behaviour of the *M*(4) and *M*(1,2,3) sites is quite different in relation to the preferred cations substituting at the different sites. Doing so brings the magnesium-iron-manganese amphiboles into line with related amphibole subgroups involving B-group Ca, Na, Li. Moreover, this view is supported by the optical data of Evans *et al.* (2001) in which there is a radical change in optical properties between the solid solutions ${}^{B}Mg_2{}^{C}Mg_5Si_8O_{22}(OH)_2$ – ${}^{B}Fe^{2+}{}_2{}^{C}Mg_5Si_8O_{22}(OH)_2$ and ${}^{B}Fe^{2+}{}_2{}^{C}Mg_5Si_8O_{22}(OH)_2$ – ${}^{B}Fe^{2+}{}_2{}^{C}Fe^{2+}{}_5Si_8O_{22}(OH)_2$ (Fig. 5).

Thus there seems to be a good scientific reason to treat Mg, Fe^{2+} and Mn^{2+} as distinct B-group constituents with regard to the classification and nomenclature of the amphiboles.

However, if we were to treat Mg, Fe^{2+} and Mn^{2+} in exactly the same way as we treat other constituents, particularly Ca, we end up with some undesirable features. For example, if we were to adhere to the dominant-constituent rule of IMA (Hatert and Burke 2008), the composition $\square(Ca_{0.53}Mg_{0.49}Fe^{2+}_{0.49}Mn^{2+}_{0.49})_{\Sigma 2}Mg_5Si_8O_{22}(OH)_2$ = $\square(Ca_{0.53}{}^{B}\Sigma M^{2+}_{1.47})_{\Sigma 2}Mg_5Si_8O_{22}(OH)_2$ would be assigned the name tremolite. Such a change is undesirable from many aspects, as it would drastically extend the compositional field of tremolite and contract the collective compositional field of the magnesium-iron-manganese amphiboles. One way around this problem is to retain the criterion used in IMA2012 for this purpose: the boundary between the calcium- and the collective magnesium-, iron- and manganese-amphibole subgroup is assigned as ${}^{B}Ca / \Sigma B \geq {}^{B}\Sigma M^{2+} / \Sigma B$, and then the individual magnesium-, iron- and manganese-amphibole subgroups are assigned as ${}^{B}Mg / \Sigma B \geq {}^{B}\Sigma Fe^{2+} / \Sigma B$, ${}^{B}\Sigma Mn^{2+} / \Sigma B$, *etc.* within the collective subgroup of the magnesium-iron-manganese amphiboles. Note that, unlike IMA2012, this new nomenclature adheres to the definition of "ferro-": ${}^{C}Fe^{2+} > {}^{C}Mg$, ${}^{C}Mn^{2+}$ except where well-established names *(i.e.* grunerite) are retained.

Nomenclature

So how should the resultant amphibole species be named (Table 9)? At the present time, there is no well-characterized monoclinic amphibole with the dominant end-member composition ${}^{A}\square{}^{B}Mg_2{}^{C}Mg_5{}^{T}Si_8O_{22}(OH)_2$. If this is assigned as the end-member formula of cummingtonite, there will be no cummingtonite known in the geological record and all the cummingtonites in the literature will be renamed "name 1" as in Table 9. Few if any mineralogists and petrologists would consider this a satisfactory procedure. It seems more practical to redefine cummingtonite as having the end-member formula ${}^{A}\square{}^{B}Fe^{2+}_2{}^{C}Mg_5{}^{T}Si_8O_{22}(OH)_2$: all amphiboles named cummingtonite in the literature will remain cummingtonite and monoclinic amphiboles with the end-member formula ${}^{A}\square{}^{B}Mg_2{}^{C}Mg_5{}^{T}Si_8O_{22}(OH)_2$ (if found) will be assigned a new name.

Current ambiguity in naming magnesium-iron-manganese amphiboles

IMA2012 contains the following statements: "The new classification presented here is based on the chemical formula of an amphibole measured by electron microprobe or wet-chemical techniques, *possibly augmented by additional analytical, structural and spectroscopic data*" (our italics). Some degree of ambiguity is introduced by the inclusion of "structural and spectroscopic data". As noted above, if we assign excess C-group cations to the B-group in the order Mn^{2+}, Fe^{2+}, then Mg, this assumes that there is no Mn^{2+} or Fe^{2+} at *M*(1,2,3). However, we have seen from the structural and spectroscopic results for cummingtonite-($P2_1/m$) that this is not the case:

some Fe^{2+} occurs at the *M*(1,2,3) sites even though $^{[6]}Mg$ exceeds 5.00 apfu. Moreover, Reece *et al.* (2000) showed that Mn^{2+} is not completely ordered at the *M*(4) site in an Fe-free *C*2/*m* cummingtonite. Thus the boundaries between the possible end-members listed in Table 9 depend on the experimental method used to determine the assignment of cations in the structure. In terms of the approval of new species, this is not a problem as use of crystal-structure refinement and spectroscopy is almost always required. However, work on the chemical characterization of amphiboles commonly involves EMPA only, and then ambiguity can arise in the naming of amphiboles with these compositions depending on the experimental techniques available to particular scientists. We can live with this ambiguity in the description and approval of new magnesium-iron-manganese amphiboles as this requires crystal-structure refinement and spectroscopy data on site occupancies. However, naming of already approved magnesium-iron-manganese amphiboles, as is the case for much compositional and petrological work on these amphiboles, assigns excess C-group cations to the B-group in the order Mn^{2+}, Fe^{2+}, then Mg, and the amphiboles are named according to the dominance of ^{B}Mg, $^{B}Fe^{2+}$ or $^{B}Mn^{2+}$. Use of EMPA data only *versus* the collective use of EMPA data, crystal structure refinement and/or spectroscopic data may result in the assignment of different names for the same material. How to resolve this ambiguity is not clear.

A major issue with naming and classifying amphiboles is striking a balance between ease of use and rigour. Overemphasis on ease of use is accompanied by the risk of misrepresenting their crystal chemistry and compromising their use in Petrology. Overemphasizing rigour restricts the effective use of amphiboles to those who have sophisticated instrumentation and expertise in its use. These opposing issues tend to lead to a split in the amphibole community, but this is not necessarily a bad thing. Two camps pulling in opposite directions will hopefully lead to solutions that are semi-acceptable to the general community.

Acknowledgements. We thank Mark Welch and Gianluca Iezzi for their excellent reviews of this paper. FCH was supported by a Tier-I Canada Research Chair in Crystallography and Mineralogy, Research Tools and Equipment, and Discovery grants from the Natural Sciences and Engineering Research Council of Canada, and by Canada Foundation for Innovation Grants for instrumentation.

Supplementary material. To view supplementary material for this article, please visit https://doi.org/...

Competing interests. The authors declare none.

References

Asklund B., Brown W.L. and Smith J.V. (1962) Hornblende-cummingtonite intergrowths. *American Mineralogist*, **47**, 160–163.

Bancroft G.M., Burns R.G. and Maddock A.G. (1967) Determination of cation distribution in the cummingtonite-grunerite series by Mössbauer spectroscopy. *American Mineralogist*, **52**, 1009–1026.

Barabanov A.V. and Tomilov S.B. (1973) Mössbauer study of the isomorphous series anthophyllite-gedrite and cummingtonite-grunerite. *Geochemistry International*, 1240–1267.

Boffa Ballaran T., Angel R.J. and Carpenter M.A. (2000) High pressure transformation behaviour of the cummingtonite-grunerite solid solution. *European Journal of Mineralogy*, **12**, 1195–1213.

Boffa Ballaran T., Carpenter M.A. and Domeneghetti M.C. (2001) Phase transitions and mixing behaviour of the cummingtonite-grunerite solid solution. *Physics and Chemistry of Minerals*, **28**, 87–101.

Boffa Ballaran T., McCammon C.A. and Carpenter M.A. (2002) Order parameter behavior at the structural phase transition in cummingtonite from Mössbauer spectroscopy. *American Mineralogist*, **87**, 1490–1493.

Boffa Ballaran T., Carpenter M.A. and Domeneghetti M.C. (2004) Order parameter variation through the *C*2/*m*-*P*2_1/*m* phase transition in cummingtonite. *American Mineralogist*, **89**, 1717–1727.

Bown M.G. (1966) A new amphibole polymorph in intergrowth with tremolite: clino-anthophyllite. *American Mineralogist*, **51**, 259–260.

Burns R.G. and Strens R.G.J. (1966) Infrared study of the hydroxyl bands in clinoamphiboles. *Science*, **153**, 890–892.

Cámara F., Oberti R., Iezzi G. and Della Ventura G. (2003) The *P*2_1/*m* « *C*2/*m* phase transition in the synthetic amphibole Na NaMg Mg_5 Si_8 O_{22} $(OH)_2$: Thermodynamic and crystal-chemical evaluation. *Physics and Chemistry of Minerals*, **30**, 570–581.

Cámara F., Oberti R., Della Ventura G., Welch M.D. and Maresch W.V. (2004) The crystal-structure of synthetic $NaNa_2Mg_5Si_8O_{21}(OH)_3$, a triclinic $C\bar{1}$ amphibole with a triple-cell and excess hydrogen. *American Mineralogist*, **89**,1464–1473.

Cámara F., Oberti R. and Casati N. (2008) The $P2_1/m \leftrightarrow C2/m$ phase transition in amphiboles: new data on synthetic amphibole $Na(NaMg)Mg_5Si_8O_{22}F_2$ and the role of differential polyhedral expansion. *Zeitschrift fűr Kristallographie*, **223**, 148–159.

Dasgupta S., Miura H. and Hariya Y. (1985) Stability of Mn-cummingtonite - an experimental study. *Mineralogical Journal*, **12**, 251–259.

Evans B.W. and Ghiorso M.S. (1995) Thermodynamics and petrology of cummingtonite. *American Mineralogist*, **80**, 649–663.

Evans B.W. and Medenbach O. (1997) The optical properties of cummingtonite and their dependence on Fe-Mg order-disorder. *European Journal of Mineralogy*, **9**, 993–1003.

Evans B.W., Ghiorso M.S., Yang H. and Medenbach O. (2001) Thermodynamics of the amphiboles: Anthophyllite-ferroanthophyllite and the ortho-clino phase loop. *American Mineralogist*, **86***,* 640–651.

Gatta G.D., McIntyre G.J., Oberti R. and Hawthorne F.C. (2017) Order of $^{[6]}Ti^{4+}$ in a Ti-rich calcium amphibole from Kaersut, Greenland: a combined X-ray and neutron diffraction study. *Physics and Chemistry of Minerals*, **44**, 83–94.

Ghiorso M.S., Evans B.W., Hirschmann M. and Yang H. (1995) Thermodynamics of the amphiboles: Fe–Mg cummingtonite solid solutions. *American Mineralogist*, **80**, 502–519.

Ghose S. and Weidner J.R. (1972) Mg^{2+}–Fe^{2+} order-disorder in cummingtonite $(Fe,Mg)_7Si_8O_{22}(OH)_2$: a new geothermometer. *Earth and Planetary Science Letters*, **16**, 346–354.

Ghose S. and Yang H. (1989) Mn-Mg distribution in a *C*2/*m* manganoan cummingtonite: Crystal-chemical considerations. *American Mineralogist*, **74**, 1091–1096.

Hafner S.S. and Ghose S. (1971) Iron and magnesium distribution in cummingtonites $(Fe,Mg)_7Si_8O_{22}(OH)_2$. *Zeitschrift für Kristallographie*, **133**, 301–326.

Hatert F. and Burke E.A.J. (2008) The IMA–CNMNC dominant-constituent rule revisited and extended. *Canadian Mineralogist*, **46**, 717–728.

Hawthorne F.C. (1983) The crystal chemistry of the amphiboles. *The Canadian Mineralogist*, **21**, 173–480.

Hawthorne F.C. (1988) Mössbauer spectroscopy. *Reviews in Mineralogy*, **18**, 255–340.

Hawthorne F.C. and Della Ventura G. (2007) Short-range order in amphiboles. *Reviews in Mineralogy and Geochemistry*, **67**, 173–222.

Hawthorne F.C. and Grundy H.D. (1976) The crystal chemistry of the amphiboles. IV. X-ray and neutron refinements of the crystal structure of tremolite. *The Canadian Mineralogist*, **14**, 334–345.

Hawthorne F.C. and Oberti R. (2007a) Amphiboles: Crystal chemistry. *Reviews in Mineralogy and Geochemistry*, **67**, 1–54.

Hawthorne F.C. and Oberti R. (2007b) Classification of the amphiboles. *Reviews in Mineralogy and Geochemistry*, **67**, 55–58.

Hawthorne F.C., Schindler M., Abdu Y., Sokolova E., Evans B.W. and Ishida K. (2008) The crystal chemistry of the gedrite-group amphiboles. II. Stereochemistry and chemical relations. *Mineralogical Magazine*, **72**, 731–745.

Hawthorne F.C., Oberti R., Harlow G.E., Maresch W., Martin R.F., Schumacher J.C. and Welch M.D. (2012) Nomenclature of the amphibole supergroup. *American Mineralogist*, **97**, 2031–2048.

Hirschmann M., Evans B.W. and Yang Hexiong (1994) Composition and temperature dependence of Fe–Mg ordering in cummingtonite-grunerite as determined by X-ray diffraction. *American Mineralogist*, **79**, 862–877.

Iezzi G., Della Ventura G., Oberti R., Cámara F. and Holtz F. (2004) Synthesis and crystal-chemistry of $Na(NaMg)Mg_5Si_8O_{22}(OH)_2$, a $P2_1/m$ amphibole. *American Mineralogist*, **89**, 640–646.

Iezzi G., Tribaudino M., Della Ventura G., Nestolo F. and Bellatreccia F. (2005a) High-T phase transition of synthetic $^{A}Na^{B}(LiMg)^{C}Mg_5Si_8O_{22}(OH)_2$ amphibole: an X-ray synchrotron powder diffraction and FTIR spectroscopic study. *Physics and Chemistry of Minerals*, **32**, 515–523.

Iezzi G., Gatta G.D., Kockelmann W., Della Ventura G., Rinaldi R., Schäfer W., Piccinini M. and Gaillard D.F. (2005b) Low-T neutron powder-diffraction and synchrotron-radiation IR study of synthetic amphibole $Na(NaMg)Mg_5Si_8O_{22}(OH)_2$. *American Mineralogist*, **90**, 695–700.

Iezzi G., Della Ventura G. and Tribaudino M. (2006) Synthetic $P2_1/m$ amphiboles in the system Li_2O-Na_2O-MgO-SiO_2-H_2O (LNMSH). *American Mineralogist*, **91**, 426–429.

Iezzi G., Della Ventura G., Tribaudino M., Nemeth P., Margiolaki I., Cavallo A., Gaillard F. and Behrens H. (2010) Phase transition induced by solid solution: The ^{B}Ca-^{B}Mg substitution in richteritic amphiboles. *American Mineralogist*, **95**, 369–381.

Iezzi G., Tribaudino M., Della Ventura G. and Margiolaki I. (2011) The high-temperature $P2_1/m \rightarrow C2/m$ phase transitions in synthetic amphiboles along the richterite–(^{B}Mg)–richterite join. *American Mineralogist,* **96***,* 353–363.

Jaffe H-W., Robinson P. and Klein C. (1968) Exsolution lamellae and optic orientation of clinoamphiboles. *Science*, **160**, 776–778.

Joplin G.A. (1942) Petrological studies in the Ordovician of New South Wales. I. The Cooma Complex. *Proceedings of the Linnean Society of New South Wales*, **67**, 157–196.

Kisch H.J. (1969) Magnesiocummingtonite-$P2_1/m$: A Ca- and Mn-poor clino-amphibole from New South Wales. *Contributions to Mineralogy and Petrology*, **21**, 319–331.

Klein C. (1964) Cummingtonite-grunerite series: a chemical, optical and X-ray study. *American Mineralogist*, **49**, 963–982.

Klein C. and Waldbaum D.R. (1967) X-ray crystallographic properties of the cummingtonite-grunerite series. *Journal of Geology*, **7**, 379–392.

Klein U., Schumacher J.C. and Czank M. (1996) Mutual exsolution in hornblende and cummingtonite: Compositions, lamellar orientations, and exsolution temperatures. *American Mineralogist*, **81**, 928–939.

Maresch W.V. and Czank M. (1983) Phase characterization of synthetic amphiboles on the join $Mn^{2+}_x\ Mg_{7-x}\ [Si_8O_{22}]\ (OH)_2$. *American Mineralogist*, **68**, 744–753.

Mueller R. (1960) Compositional characteristics and equilibrium relations in mineral assemblages of a metamorphosed iron formation. *American Journal of Science*, **258**, 449–497.

Papike J.J. and Ross M. (1970) Gedrites: crystal structures and intracrystalline cation distributions. *American Mineralogist*, **55**, 1945–1972.

Papike J.J., Ross M. and Clark J.R. (1969) Crystal chemical characterization of clinoamphiboles based on five new structure refinements. *Mineralogical Society of America Special Paper*, **2**, 117–136.

Prewitt C.T., Papike J.J. and Ross M. (1970) Cummingtonite: A reversible nonquenchable transition from $P2_1/m$ to $C2/m$ symmetry. *Earth and Planetary Science Letters*, **8**, 448–450.

Rabbitt J.C. (1948) A new study of the anthophyllite series. *American Mineralogist*, **33**, 263–323.

Rancourt D.G. and Ping J.Y. (1991) Voigt-based methods for arbitrary-shape static hyperfine parameter distributions in Mössbauer spectroscopy. *Nuclear Instruments and Methods in Physics Research Section B: Beam Interactions with Materials and Atoms*, **58**, 85–91.

Reece J.J., Redfern S.A.T, Welch M.D. and Henderson C.M.B. (2000) Mn-Mg disordering in cummingtonite: A high-temperature neutron powder diffraction study. *Mineralogical Magazine*, **64,** 255–266.

Reece J.J., Redfern S.A.T, Welch M.D., Henderson C.M.B and McCammon C.A. (2002) Temperature-dependent Fe^{2+}–Mn^{2+} order–disorder behaviour in amphiboles. *Physics and Chemistry of Minerals*, **29**, 562–570.

Robinson P. and Jaffe H.W. (1969) Chemographic exploration of amphibole assemblages from central Massachusetts and southwestern New Hampshire. *Mineralogical Society of America Special Paper*, **2**, 251–274.

Robinson P., Ross M. and Jaffe H.W. (1971) Composition of the anthophyllite-gedrite series, comparisons of gedrite-hornblende, and the anthophylite-gedrite solvus. *American Mineralogist*, **56**, 1004–1041.

Ross M., Papike J.J. and Shaw K.W. (1969) Exsolution textures as indicators of sub solidus thermal histories. *Mineralogical Society of America Special Paper*, **2**, 275–299.

Roy S. (1981) *Manganese Deposits*. Academic Press.

Schindler M., Sokolova E., Abdu Y., Hawthorne F.C., Evans B.W. and Ishida K. (2008) The crystal chemistry of the gedrite-group amphiboles. I. Crystal structure and site populations. *Mineralogical Magazine*, **72**, 703–730.

Seifert F. (1978) Equilibrium Mg-Fe^{2+} cation distribution in anthophyllite. *American Journal of Science*, **278**, 1323–1333.

Sheldrick G.M. (2008) A short history of SHELX. *Acta Crystallographica*, **A64**, 112–122.

Strens R.G.J. (1974) The common chain, ribbon, and ring silicates. Pp. 305–330 in: *The Infrared Spectra of Minerals* (V.C. Farmer, ed.). Mineralogical Society, London, UK.

Sueno S., Papike J.J., Prewitt C.T. and Brown G.E. (1972) Crystal chemistry of high cummingtonite. *Journal of Geophysical Research*, **77**, 5767–5777.

Viswanathan K. and Ghose S. (1965) The effect of Mg^{2+}–Fe^{2+} substitution on the cell dimensions of cummingtonites. *American Mineralogist*, **50**, 1106–1112.

Welch M.D., Camara F., Della Ventura G. and Iezzi G. (2007) Non-ambient *in-situ* studies of amphiboles. *Reviews in Mineralogy and Geochemistry*, **67**, 223–260.

Winchell A.N. (1938) The anthophyllite and cummingtonite-grunerite series. *American Mineralogist*, **23**, 329–333.

Wojdyr M. (2010) Fityk: a general-purpose peak fitting program. *Journal of Applied Crystallography***, 43**, 1126–1128.

Yang H. and Hirschmann M.M. (1995) Crystal structure of $P2_1/m$ ferromagnesian amphibole and the role of cation ordering and composition in the $P2_1/m$–$C2/m$ transition in cummingtonite. *American Mineralogist*, **80**, 916–922.

Yang H. and Smyth J.R. (1996) Crystal structure of a $P2_1/m$ ferromagnesian cummingtonite at 140 K. *American Mineralogist*, **81**, 363–368.

Yang H., Hazen R.M., Prewitt C.T., Finger L.W., Lu R. and Hemley R.J. (1998) High-pressure single-crystal X-ray diffraction and infrared spectroscopic studies of the $C2/m$–$P2_1/m$ phase transition in cummingtonite. *American Mineralogist*, **83**, 288–299.

Figure captions

Fig. 1. The $P2_1/m$ amphibole structure projected onto (100); polyhedra: *T*(1A) = bright yellow, *T*(2A) = bright green, *T*(1B) = pale yellow, *T*(2B) = pale green, *M*(1) = mauve, *M*(2) = blue, *M*(3) = red; sites: *M*(4) = blue circle.

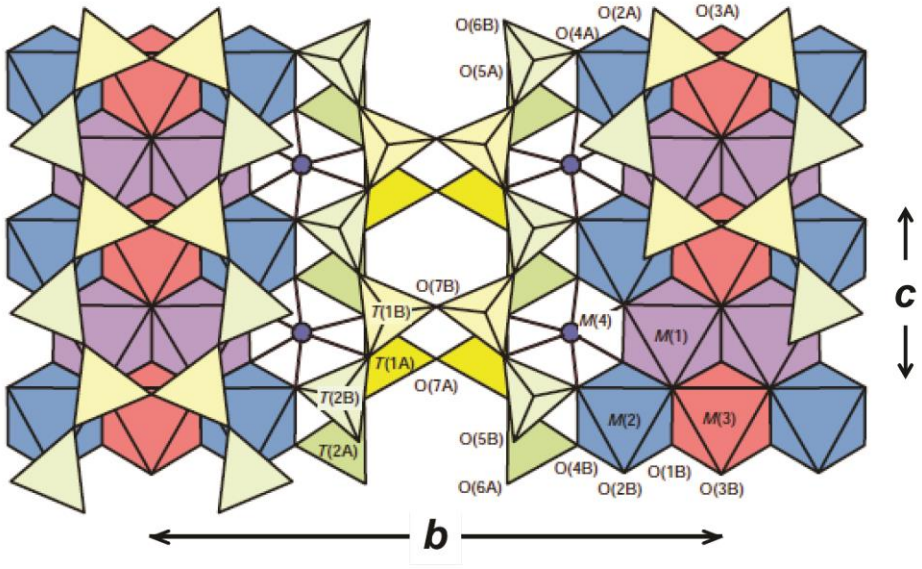

Fig. 2 The infrared spectrum of cummingtonite-($P2_1/m$) in the principal (OH)-stretching region.

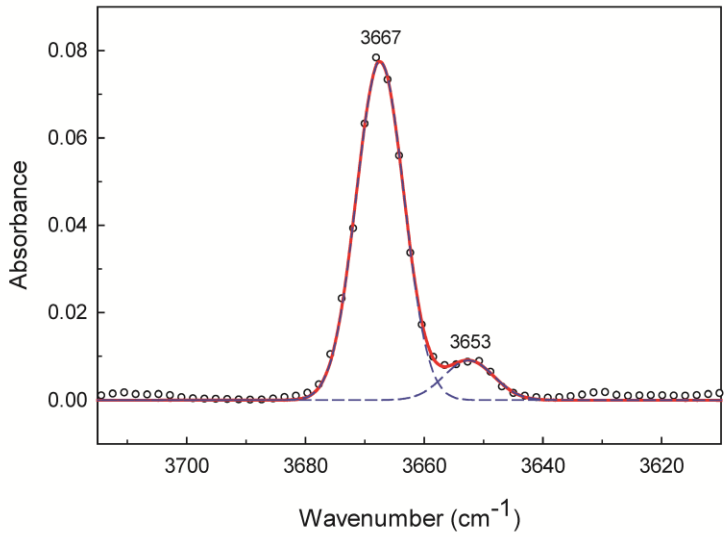

Fig. 3. The ^{57}Fe Mössbauer spectrum of cummingtonite-($P2_1/m$). Blue doublet: Fe^{2+} at $M(4)$; green doublet: Fe^{2+} at $M(1,2,3)$; red doublet: Fe^{3+} at $M(2)$ in exsolution lamellae.

3

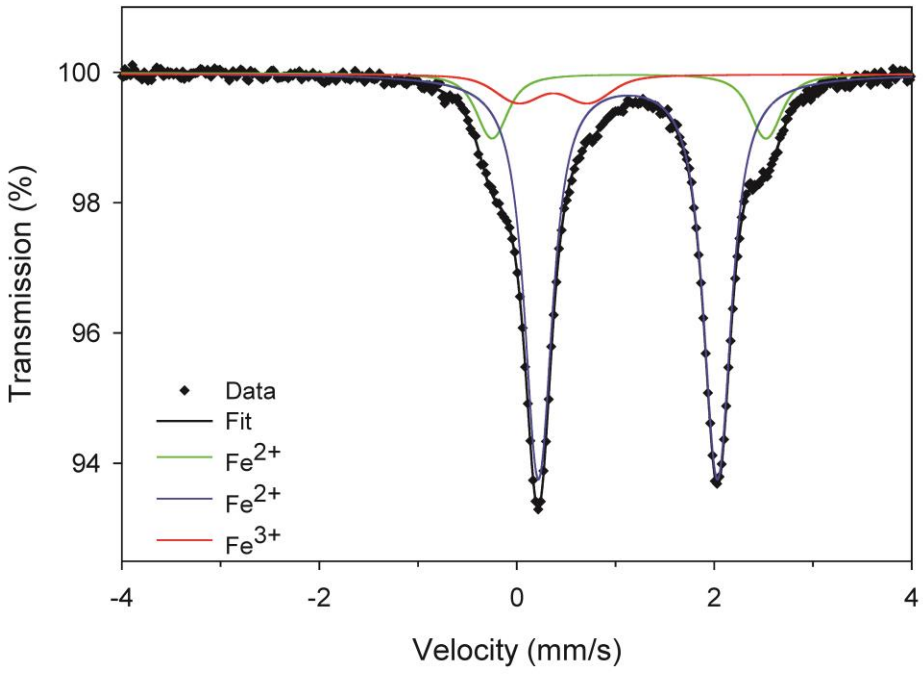

Fig. 4. Order of Fe^{2+} and Mg between the *M*(4) and *M*(1,2,3) sites in monoclinic low-Mn magnesium-iron-manganese amphiboles. The red triangles are the unheated data of Hirschmann *et al*. (1994) and the green circle is the data of cummingtonite-($P2_1/m$) from this work. IMA2012 treats these compositions as having no order of Mg and Fe^{2+} between the B- and C-groups of cations [*i.e*. the *M*(4) and *M*(1,2,3) sites], and according to this model, the data should follow the straight dashed black line labelled IMA2012. An alternative model is to assume complete order of Fe^{2+} and Mg between the B- and C-groups of cations [*i.e*. the *M*(4) and *M*(1,2,3) sites], as indicated by the solid green lines that more closely approximate the experimental data.

4

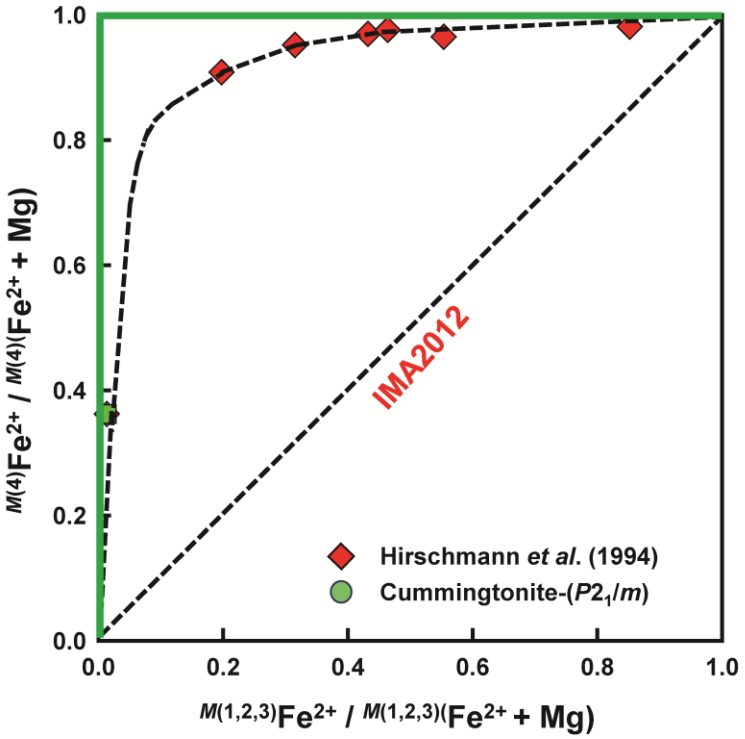

Fig. 5. Variation of $2V_z$ of anthophyllite-ferroanthophyllite (hollow circles) and metamorphic cummingtonite-grunerite (solid circles) as a function of (Fe + Mn) / (Fe + Mn + Mg); modified from Evans *et al.* (2001).

5

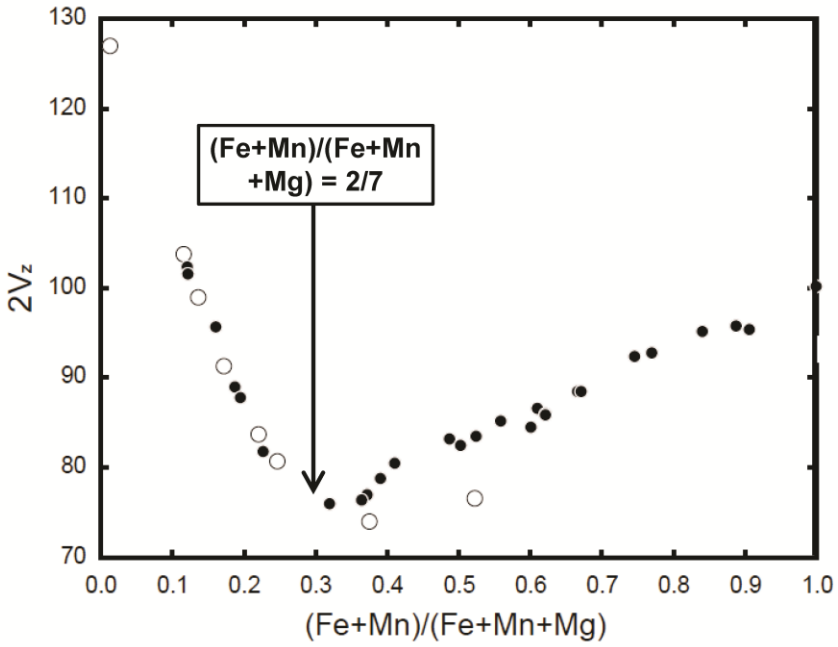

Table 1. Chemical composition (wt%)* and unit formula (apfu) for cummingtonite-($P2_1/m$).

	wt%		apfu
SiO_2	56.4	Si	7.86
Al_2O_3	0.7	Al	0.11
TiO_2	0.04	Σ	7.97
FeO	10.8		
MnO	0.55	Ti^{4+}	0.00
MgO	26.85	Fe^{2+}	1.26
CaO	0.95	Mn^{2+}	0.06
Na_2O	0.4	Mg	5.57
H_2O	2.16	Ca	0.14
Σ	98.85	Σ	7.03
		Na	0.11
		(OH)	2.00

*Chemical composition from Kisch (1969).

Table 2. Infrared band positions, observed intensities and associated local arrangements for cummingtonite-($P2_1/m$).

Band	Frequency (cm^{-1})	Intensity (a.u.)	Local arrangement
A	3667.5	0.778	MgMgMg–(OH)–$^{A}\square$
B	3652.5	0.095	MgMgFe^{2+}–(OH)–$^{A}\square$

Table 3. Mössbauer parameters for cummingtonite-($P2_1/m$).

Site	CS* (mm/s)	QS** (mm/s)	A*** (%)
$^{M(4)}Fe^{2+}$	1.13	1.81	78
$^{M(1,2,3)}Fe^{2+}$	1.14	2.77	14
Fe^{3+}	0.37	0.71	8

*CS = Centre Shift relative to α–Fe at RT; sd = 0.02 mm/s;
**QS = Quadrupole Splitting; sd = 0.02 mm/s;
***A = relative area; sd = 1%.

Table 4. Miscellaneous information for cummingtonite-($P2_1/m$).

a (Å)	9.4885(19)	crystal size (μm)	80 x 40 x 35
b	18.040(4)	radiation/monochromater	Mo*K*α/Graphite
c	5.2891(11)	Total no. of reflections	10392
β (°)	102.06(3)	No. unique reflections	2684
V (Å^3)	885.4(3)	No. $I_o > 4\sigma I$	2338
Sp. Gr.	$P2_1/m$	R_{int} %	1.75
Z	2	R_{obs} %	3.34
D_{calc} (g/cm^3)	3.093	R_{all} %	3.78

Table 5. Site coordinates and anisotropic-displacement parameters for cummingtonite-($P2_1/m$).

Site	x	y	z	U^{11}	U^{22}	U^{33}	U^{23}	U^{13}	U^{12}	U_{eq}
M(1)	0.74982(7)	0.33661(4)	0.48749(13)	0.0082(4)	0.0062(4)	0.0065(4)	–0.0003(2)	0.0016(3)	–0.0003(2)	0.0070(3)
M(2)	0.74993(7)	0.42679(4)	0.98671(11)	0.0081(4)	0.0064(4)	0.0067(4)	–0.0002(2)	0.0015(3)	–0.0002(3)	0.0072(2)
M(3)	0.75077(10)	¼	0.98916(18)	0.0072(6)	0.0060(6)	0.0063(6)	0	0.0011(4)	0	0.0066(4)
M(4)	0.74793(4)	0.50913(2)	0.48383(7)	0.0100(2)	0.0109(2)	0.0086(2)	–0.00033(14)	0.00430(15)	–0.00119(14)	0.00947(16)
T(1A)	0.03918(6)	0.33448(3)	0.26062(11)	0.0058(3)	0.0053(3)	0.0061(3)	–0.00006(18)	0.0011(2)	–0.00042(18)	0.00575(14)
T(1B)	0.53754(6)	0.83377(3)	0.28763(11)	0.0067(3)	0.0057(3)	0.0061(3)	0.00003(18)	0.0013(2)	–0.00015(19)	0.00616(14)
T(2A)	0.04586(6)	0.42029(3)	0.76648(11)	0.0062(3)	0.0062(3)	0.0059(3)	–0.00011(18)	0.0014(2)	–0.00091(19)	0.00607(14)
T(2B)	0.54926(6)	0.91829(3)	0.79317(11)	0.0071(3)	0.0069(3)	0.0063(3)	–0.00029(18)	0.0016(2)	–0.0012(2)	0.00674(14)
O(1A)	0.86506(16)	0.33652(8)	0.1997(3)	0.0067(7)	0.0067(7)	0.0077(6)	–0.0002(5)	0.0017(5)	–0.0003(5)	0.0070(3)
O(1B)	0.36350(16)	0.83667(8)	0.2206(3)	0.0061(7)	0.0066(7)	0.0093(7)	–0.0002(5)	0.0015(5)	–0.0000(5)	0.0073(3)
O(2A)	0.87121(16)	0.42226(9)	0.7025(3)	0.0064(7)	0.0085(7)	0.0080(6)	0.0000(5)	0.0017(5)	–0.0003(5)	0.0076(3)
O(2B)	0.37408(16)	0.92277(9)	0.7316(3)	0.0065(7)	0.0095(7)	0.0091(7)	–0.0001(5)	0.0018(5)	–0.0001(5)	0.0083(3)
O(3A)	0.8641(2)	¼	0.6971(4)	0.0067(10)	0.0081(10)	0.0092(9)	0	0.0012(8)	0	0.0081(4)
O(3B)	0.3621(2)	¾	0.7191(4)	0.0066(10)	0.0092(10)	0.0097(9)	0	0.0021(8)	0	0.0085(4)
O(4A)	0.12701(17)	0.49837(9)	0.7841(3)	0.0096(7)	0.0075(7)	0.0097(7)	–0.0005(5)	0.0015(5)	–0.0032(5)	0.0090(3)
O(4B)	0.63325(17)	0.99352(9)	0.7592(3)	0.0120(7)	0.0092(7)	0.0105(7)	0.0011(5)	0.0020(6)	–0.0039(6)	0.0106(3)
O(5A)	0.10067(17)	0.37178(9)	0.0274(3)	0.0083(7)	0.0175(8)	0.0113(7)	0.0079(6)	0.0030(5)	0.0004(6)	0.0122(3)
O(5B)	0.60220(16)	0.88787(9)	0.0914(3)	0.0084(7)	0.0119(7)	0.0081(7)	0.0037(5)	0.0012(5)	–0.0016(6)	0.0095(3)
O(6A)	0.10457(17)	0.38050(9)	0.5247(3)	0.0086(7)	0.0169(8)	0.0101(7)	–0.0065(6)	0.0011(5)	0.0013(6)	0.0120(3)
O(6B)	0.59754(17)	0.86035(9)	0.5854(3)	0.0090(7)	0.0151(8)	0.0086(7)	–0.0042(6)	0.0005(5)	0.0027(6)	0.0111(3)

O(7A)	0.0967(2)	¼	0.2980(5)	0.0075(10)	0.0053(9)	0.0192(11)	0	0.0009(8)	0	0.0110(4)
O(7B)	0.5933(2)	¾	0.2568(4)	0.0103(10)	0.0057(9)	0.0141(10)	0	0.0025(8)	0	0.0100(4)
HA	0.964(2)	¼	0.768(9)	0.03						
HB	0.465(2)	¾	0.769(10)	0.03						

Table 6. Selected interatomic distances (Å) in cummingtonite-($P2_1/m$).

T(1A)–O1A	1.616(2)	*T*(1B)–O1B	1.616(2)
T(1A)–O5A	1.617(2)	*T*(1B)–O5B	1.632(2)
T(1A)–O6A	1.632(2)	*T*(1B)–O6B	1.631(2)
T(1A)–O7A	1.617(1)	*T(*1B)–O7B	1.621(1)
<*T*(1A)–OA>	1.621	<*T*(1B)–OB>	1.625
T(2A)–O2A	1.621(2)	*T*(2B)–O2B	1.628(2)
T(2A)–O4A	1.599(2)	*T*(2B)–O4B	1.603(2)
T(2A)–O5A	1.625(3)	*T*(2B)–O5B	1.650(2)
T(2A)–O6A	1.661(2)	*T*(2B)–O6B	1.649(2)
<*T(*2A)–OA>	1.626	<*T*(2B)–OB>	1.632
M(1)–O1A	2.051(2)	*M*(2)–O1A	2.145(2)
M(1)–O1B	2.058(2)	*M*(2)–O1B	2.124(2)
M(1)–O2A	2.112(2)	*M*(2)–O2A	2.077(2)
M(1)–O2B	2.138(2)	*M*(2)–O2B	2.084(2)
M(1)–O3A	2.084(2)	*M*(2)–O4A	2.016(2)
M(1)–O3B	2.068(2)	*M*(2)–O4B	2.046(2)
<*M*(1)–O>	2.085	<*M*(2)–O>	2.082
M(3)–O1A	2.085(2) x2	*M*(4)–O2A	2.144(2)
M(3)–O1B	2.086(2) x2	*M*(4)–O2B	2.125(2)
M(3)–O3A	2.058(3)	*M*(4)–O4A	2.034(2)
M(3)–O3B	2.054(3)	*M*(4)–O4B	1.992(2)
<*M*(3)–O>	2.075	*M*(4)–O6A	2.440(2)
		M(4)–O6B	2.862(2)
O3A–HA	0.94(2)	HA–O5A	2.77(2) x2
		HA–O7A	2.83(2)
O3B–HB	0.96(2)	HB–O6B	2.65(2) x2
		HB–O7B	2.61(2)

Table 7. Assigned site populations (apfu) for cummingtonite-($P2_1/m$).

Site	Site population (apfu)
T(1A)	2.00 Si
T(1B)	2.00 Si
T(2A)	2.00 Si
T(2B)	2.00 Si
M(1)	1.972(8) Mg + 0.028 Fe^{2+}
M(2)	2.000 Mg
M(3)	0.989(6) Mg + 0.011 Fe^{2+}
M(4)	0.815(8) Mg + 1.125 Fe^{2+} + 0.060 Mn^{2+}

Table 8. Mean OH-M distances (Å) and peaks (cm^{-1}) in the principal OH-stretching region of the infrared for selected amphiboles.

	<O3A–Mg_3> Å	<O3B–Mg_3> Å	Ref.
$^{A}Na^{B}(LiMg)^{C}Mg_5Si_8O_{22}(OH)_2$	---	---	
OH-peaks: position and half-width (cm^{-1})	3748 24	3712 14	(1)
$Na(NaMg)Mg_5Si_8O_{22}(OH)_2$	1.996	2.130	
OH-peaks: position and half-width (cm^{-1})	3751 27	3718 12	(2)
Cummingtonite-($P2_1/m$)	2.075	2.063	
OH-peaks: position and half-width (cm^{-1})	3667 10		(3)
Cummingtonite-($C2/m$)	2.061		
OH-peaks: position and half-width (cm^{-1})	3666 8		(4)

References: (1) Iezzi *et al.* (2005a); (2) Iezzi *et al.* (2005b); (3) This work; (4) Reece *et al*. (2000).

Table 9. Possible end-member schemes for magnesium-iron-manganese amphiboles.

IMA2012	
Cummingtonite	$\square Mg_2Mg_5Si_8O_{22}(OH)_2$
Grunerite	$\square Fe^{2+}_2Fe^{2+}_5Si_8O_{22}(OH)_2$
Rootname 3	$\square Mn^{2+}_2Mg_5Si_8O_{22}(OH)_2$
Ferro-rootname 3	$\square Mn^{2+}_2Fe^{2+}_5Si_8O_{22}(OH)_2$
Mangano-rootname 3	$\square Mn^{2+}_2Mn^{2+}_5Si_8O_{22}(OH)_2$
Possible new end-members	
(1) Name1	$\square Mg_2Mg_5Si_8O_{22}(OH)_2$
(2) Name2	$\square Fe^{2+}_2Mg_5Si_8O_{22}(OH)_2$
(3) Name3	$\square Mn^{2+}_2Mg_5Si_8O_{22}(OH)_2$
Grunerite	$\square Fe^{2+}_2Fe^{2+}_5Si_8O_{22}(OH)_2$
Ferro-name3	$\square Mn^{2+}_2Fe^{2+}_5Si_8O_{22}(OH)_2$
Mangano-name3	$\square Mn^{2+}_2Mn^{2+}_5Si_8O_{22}(OH)_2$